Spinal motoneurone distress during experimental allergic encephalomyelitis

L. Giardino*†, A. Giuliani*, M. Fernandez* and L. Calzà*†

*Department of Veterinary Morphophysiology and Animal Production (DIMORFIPA), University of Bologna, Ozzano dell'Emilia, and †Pathophysiology Center for the Nervous System, Hesperia Hospital, Modena, Italy

L. Giardino, A. Giuliani, M. Fernandez and L. Calzà (2004) *Neuropathology and Applied Neurobiology*, **30**, 522–531

Spinal motoneurone distress during experimental allergic encephalomyelitis

The main pathophysiological feature characterizing multiple sclerosis (MS) is demyelination. However, the possibility of neural damage has recently been proposed as a mechanism in chronic disease. Experimental allergic encephalomyelitis (EAE) is the most widely used experimental model for MS. We investigated occurrences of microglial activation and astrocytosis in the spinal cord, choline acetyl-transferase (ChAT) and calcitonin gene-related peptide (CGRP) mRNA regulation in spinal motoneurones during EAE. EAE was induced in female Lewis rats by injecting guinea pig spinal cord tissue in complete Freund's adjuvant (CFA) to which heat-inactivated Mycobacterium had been added. Rats injected with CFA and uninjected rats were used as controls. ChAT and CGRP mRNAs were studied by *in situ* hybridization in the lumbar spinal cord and a computerized grain counting procedure was used for quantification. No differences in ChAT mRNA level were found between control and CFA-injected rats. ChAT mRNA level was strongly reduced in EAE 14 days after immunization and then recovered (29 days after immunization). CGRP mRNA increased 14 days after immunization, and then recovered to control level. Extensive long-lasting gliosis developed in the spinal cord and around motoneurones and a transient expression of p75$^{\text{LNGFR}}$ in motoneurones was also found. These data suggest that during EAE, gliosis induces distress in spinal cord neurones involving the synthesis enzyme for the main transmitter.

Keywords: demyelinating disease, inflammation, nerve growth factor, neurone, spinal cord

Introduction

Multiple sclerosis (MS) is a demyelinating disease characterized by extensive inflammation and gliosis in the central nervous system [1]. The main pathological feature of MS is widespread demyelination and oligodendrocyte degeneration [2]. MS has therefore been interpreted as an oligodendrocyte disease. More recently, the possibility of neural damage has been raised. In particular, it is accepted that axonal loss occurs in different areas of the central nervous system [3,4] including the spinal cord [5] and corpus callosum [6]; this lesion is involved in permanent disability characterizing the later chronic progressive stage of MS [7–9]. Magnetic resonance imaging (MRI), magnetic resonance spectroscopy (MRS) and MRS imaging studies have provided evidence that axonal loss and neural damage in MS can be both substantial and early [10,13] and these noninvasive measures have demonstrated the existence of direct links between these axonal changes and disability [14–16].

Histopathological studies have confirmed this clinical evidence, indicating that both atrophy and decreased density contribute to substantial axonal loss in brain and spinal cord [5,17] and that the highest incidence of acute axonal injury is found during active demyelination [18], as well as in patients with secondary progressive MS [3].

Correspondence: Prof. L. Calzà, DIMORFIPA, Università di Bologna, Via Tolara di Sopra 50, 40064 Ozzano dell'Emilia, Italy. Tel: + 39-051-2097947; Fax: + 39-051-2097953; E-mail: lcalza@vet.unibo.it

Evidence from work on animals has also demonstrated that damage to axons can occur with central nervous system inflammation, as indicated in mice infected with a neurotropic coronavirus [19], in experimental allergic encephalomyelitis (EAE) [18,20,21] and in nonhuman primate models of MS [22].

Neuroprotection has consequently come to be considered a possible strategy for MS patients [8,23]. However, development of neuroprotective strategies is dependent on defining the precise mechanism whereby effector cells and molecules damage axons, and on whether neural damage is limited to the axon or also involves the soma. On the basis of behavioural data indicating severe neurological disabilities, including force deficit and diffuse tissue inflammation and gliosis in the spinal cord of rats affected by EAE, we investigated the relation between clinical profile, gliosis and motoneurone neurochemical phenotype in the spinal cord of EAE-affected rats. We focused on the acetylcholine synthesis enzyme [choline acetyltransferase (ChAT)], calcitonin gene-related peptide (CGRP), which is considered a trophic peptide for motoneurones, and nerve growth factor (NGF) low-affinity receptor p75^{LNGFR}, which normally is not expressed by motoneurones in adult animals. Alterations of all these markers have been described in different experimental conditions associated with axonal damage [24].

Materials and methods

Animals

Female pathogen-free Lewis rats, 150–175 g body weight (Charles River, Italy) were used. A group of rats was sensitized with a medium containing 0.15 g/ml guinea pig spinal cord tissue in complete Freund's adjuvant (CFA, Sigma, St. Louis, MO, USA), 50% v/v to which 5 mg/ml of heat-inactivated Mycobacterium (H37Ra Difco, Detroit, MI, USA) was added. A further group of rats was injected with CFA + heat-inactivated Mycobacterium. Uninjected rats were also used as controls. Rats were regularly weighed and examined for clinical signs of EAE up to 79 days after immunization by a trained observer and scored on a neurological disability scale according to which grade 1 = loss of tail tone; grade 2 = weakness in one or both hind legs or middle ataxia; grade 3 = ataxia or paralysis; grade 4 = severe hind leg paralysis; grade 5 = severe hind leg paralysis accompanied by urinary incontinence. Uninjected and CFA-injected rats were rated

as O in all observations. In all experiments, groups of EAE animals were sacrificed at 14, 21 and 79 days after immunization, adjuvant-injected animals at 14 and 79 days after sensitization, and control animals 79 days after inclusion in the experiment.

All animal protocols described herein were carried out according to the European Community Council Directives of 24 November 1986 (86/609/EEC) and approved by our intramural committee and the Italian Health Ministry, in compliance with the guidelines published in the *NIH Guide for the Care and Use of Laboratory Animals*.

Immunohistochemistry and quantification

For immunocytochemical experiments, five to six animals in each experimental group were sacrificed at set times. Animals deeply anaesthetized with ketamine (Ketalar, Parke Davis, Italy) 10 mg/kg of body weight, i.p. + diazepam 2 mg/kg, i.m., were perfused through the ascending aorta with 100 ml (50 ml at 37°C, 50 ml ice cold) Tyrode-Ca^{++}, pH 6.9, followed by 4% paraformaldehyde in Sorensen phosphate buffer 0.1 M pH 7.0 for 25–30 min. During perfusion the animals were bathed in ice-cold water. The brain and spinal cord were then removed and immersed for 2 h in ice-cold fixative, before rinsing for 48 h in ice-cold 0.1 M phosphate buffer. For immunocytochemistry, the following antisera were used: mouse antiglial fibrillary acid protein (GFAP) (Chemicon Temecula, CA, USA), mouse anti-nestin (BD PharMingen, San Jose, CA, USA), mouse anti-rat CD11b (OX42, Sera-Laboratory, Crawley Down, UK), mouse anti-oligodendrocytes (Chemicon Temecula; immunogen: oligodendrocytes cultured by the rat olfactory bulb), goat antip75^{LNGFR} (Santa Cruz Biotechnology, Inc., Santa Cruz, CA, USA). For immunofluorescence experiments, tissue was fast frozen in CO$_2$ and cut on a Leitz cryostat (thickness of section 14 µm, −20°C). Sections were first incubated in 0.1 M phosphate-buffered saline (PBS) at room temperature for 10–30 min, followed by incubation at 4°C for 48 h in a humid atmosphere with the primary antibody diluted in PBS containing 0.3% Triton X-100, v/v. Staining specificity was assessed by *in vitro* overnight preincubation of the antiserum with the respective antigen (100 µg of antigen/ ml diluted antiserum). This treatment prevented staining. After rinsing in PBS for 30 min (3 × 10 min), the sections were incubated at 37°C for 120 min in a humid atmosphere with fluoresceine isothiocyanate-conjugated anti-mouse or anti-goat immunoglobulin (Dako, Glostrup,

Denmark) containing 0.3% Triton X-100. For double experiments, two primary antisera raised in different animal species and appropriate secondary antisera were applied concomitantly. Sections were then rinsed in PBS (as above), mounted in glycerol and PBS (3 : 1, v/v) containing 1,4-phenylendiamine, 0.1 g/l. They were then examined using a Nikon Microphot FXA microscope.

For the avidin-biotin complex (ABC) technique, vibratome sections (50 μm thickness) were immediately processed for the ABC technique according to a free-floating procedure. In each experiment, sections from all animals were run in the same assay. Sections were first incubated in 0.1 M PBS at room temperature for 10–30 min, pretreated with H_2O_2 to quench endogenous peroxidase activity and then incubated with 1.5–2.0% normal serum, followed by overnight incubation at 4°C with the primary antisera diluted in PBS containing 0.3% Triton X-100, v/v. Sections were rinsed in PBS for 30 min (3×10 min) and then incubated with biotinylated antimouse or antigoat immunoglobulin (Dako); they were rinsed again in PBS and finally incubated using streptavidin biotinylated horseradish peroxidase complex (Amersham, Little Chalfont, UK) 1 : 250. Diaminobenzidine (0.5 mg/ml in Tris HCl 0.1 M pH 7.5 + H_2O_2 0.03%) was used to detect the immunocomplex. Preparations were then examined using a Nikon Microphot FXA microscope and Tmax 400 film (Kodak, Hemel Hempstead, UK) was used for photography. Color slides were then loaded via Nikon SuperCool Scan 4000 and Figure 2 was generated using Adobe Photoshop 6.0 software.

Quantification of immunocytochemical staining for glial reaction was carried out on an immunofluorescence preparation using the analytical imaging station (AIS) (Imaging Research Inc., St. Catharines, Canada). Three animal/group/times were used and six sections from the lumbar spinal cord were analysed in each animal. In each case, the ventral horn on both sides, including layers 8 and 9, was analysed in order to evaluate the percentage immunoreactive area of each antigen [25,26]. Briefly, a contrast-enhancing procedure was first applied to clearly identify the edge of immunoreactive cells. A threshold procedure was then applied to sample the immunoreactive area over the entire sampled area (% area). The average values from each animal were used for statistical analysis. Spinal cord inflammation was then scored on the same section after toluidine blue contro-staining according to Hickey *et al.* [27] using a previously described computerized image analysis procedure [28] in which

1 = occasional mononuclear cells; 2 = sparse cellular infiltrate; 3 = large patches of infiltrate with numerous mononuclear cells; 4 = dense accumulation of mononuclear cells.

In situ hybridization

Four to five animal/group/times were used for *in situ* hybridization experiments. Animals were sacrificed by decapitation, the spinal cord was quickly dissected out and frozen using CO_2. Coronal sections were cut in a cryostat from L5 and collected on ProbeOn microscope slides (Fisher Scientific, Pittsburg, PA, USA). Oligonucleotide probes complementary to mRNAs encoding ChAT (nucleotides 1818–1860) and αCGRP 664–698, respectively, were synthesized in a Beckmann OLIGO 1000 DNA synthesizer (Fullerton, CA, USA). The oligonucleotide probes were labelled at the 3′-end with α-^{35}S-dATP (New England Nuclear, Boston, MA, USA) using terminal deoxynucleotidyltransferase (Amersham) in a buffer containing 10 mM $CoCl_2$, 1 mM dithiothreitol (DTT), 300 mM Tris base, and 1.4 M potassium cacodylate (pH 7.2). Afterwards, the labelled probes were purified through Nensorb-20 columns (New England Nuclear), and DTT was added to obtain a final concentration of 10 mM. The resulting specific activity ranged from 1 to 4×10^6 dpm/ng oligonucleotide. The sections were brought to room temperature, air dried, covered with a hybridization buffer containing 50% formamide, $4 \times$ SSC ($1 \times$ SSC: 0.15 M NaCl, 0.015 M sodium citrate), $1 \times$ Denhardt's solution (0.02% polyvinyl-pyrrolidone, 0.02% bovine serum albumin and 0.02% Ficoll), 1% sarcosyl, 0.02 M phosphate buffer (pH 7.0), 10% dextran sulphate, 500 mg/ml heat-denatured salmon sperm DNA, and 200 mM DTT and 40 ng/ml of the labelled probes [29]. The slides were placed in a humid chamber and incubated for 15–20 h at 50°C. The sections were then rinsed in $1 \times$ SSC at 55°C for 1 h with six changes and washed in the same buffer for 1 h at room temperature. Finally, the slides were rinsed in distilled water followed by 60% and 95% ethanol (2 min each), air dried and then dipped in NTB2 nuclear track emulsion (Kodak) for 3 weeks before being developed with Kodak D19 for 3 min and fixed with G333 (Agfa Gevaert, Leverkusen, Germany) for 10 min. Quantitative analysis was performed on emulsion-dipped sections, slightly counterstained with toluidine blue using AIS (Imaging Research Inc.) grain counting software. ChAT and CGRP mRNAs expression was measured in the motoneurones on

both sides in the ventral horn of the spinal cord, in an area corresponding to the lateral motor nucleus, by choosing five matching sections in each animal. Eight to 10 cells on each side were then measured. Cells were considered labelled if the silver grains were more than five times the background silver level, as determined by averaging grain counts over defined areas of the spinal cord devoid of positively labelled cell bodies. The average values from each animal were used for statistical analysis.

Statistical analysis

One-way analysis of variance (ANOVA) was used, followed by Dunnet's test and Student's *t*-test.

Results

Experimental animals

Clinical profiles expressing neurological disabilities in EAE and body weight of experimental animals are reported in Figure 1. The severity of EAE gradually increases, reaches its peak between 8 and 14 days after immunization and then partially recovers. Body weight growth stops at a point corresponding to the acute phase of the disease. The growth curve then recovers but the body weight of the experimental animals remains significantly lower than control animals. In our experience [28], as confirmed in this experiment, the disease relapses with lower severity in 60% of animals. Only relapsing animals have been included in the study.

Glial activation in the spinal cord

As described in previous reports [28,30] and confirmed in this study (images not shown), in only a few rats were small scattered areas of inflammation (1–2 according to Hickey *et al.*) [27] observed 14 days after immunization. Conversely, severe inflammatory cellular infiltrate, mainly composed by mononuclear cells, appeared in many areas of the brain and spinal cord between 14 and 20 days after myelin immunization. Almost all EAE animals showed a histological picture scored as 4. Histopathological examination of EAE relapsing animals evidenced multiple, confluent foci of inflammation in both the white and the grey matter of the spinal cord, where also necrosis was observed (scored 3–4 according to Hickey *et al.* 1983) [27].

Glial cells in brain and spinal cord of EAE and control animals were studied using OX42 as marker for activated microglial cells, GFAP as marker for astrocytes and nestin as marker for activated and/or newly generated astrocytes (Figure 2). Starting from day 14 after immunization, a disaggregation of white matter bundles in the spinal cord was observed in EAE animals, which worsened during clinical remission and relapse. Images in Figure 2**A** and **B** refer to immunostaining for oligodendrocyte in longitudinal sections of the lumbar spinal cord, showing posterior funiculus and grey matter of the ventral horn in control (**A**) and EAE animals, 79 days after immunization (**B**). OX42-IR microglial cells are evident 21 days after immunization and then decline as expected in the transient activation of these cells. Nestin-positive elements, which are small,
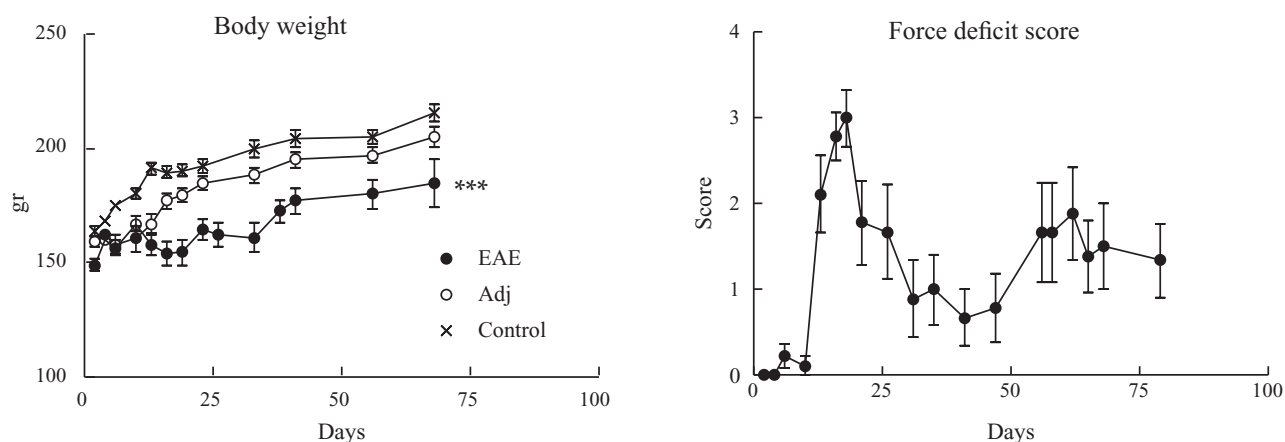
Figure 1. The time course of body weight increase and neurological disability scores in experimental animals. Data are expressed as mean ± SEM, ***$P < 0.001$.
EAE, experimental allergic encephalomyelitis; Adj, adjuvant-injected.

finely and richly branched cells (Figure 2**G,H,N**), appear as early as 14 days after immunization, for example, at a disease stage in which cellular inflammation is not yet pre-eminent (Figure 2**C**), and then decline (Figure 2**D**, 21 days after injection). GFAP-IR is higher in EAE animals 21 days after immunization than in controls and further increases in relapsing animals, where an intense astrocytosis is observed around motoneurones in the ventral horn (Figure 2**E**, control; Figure 2**F**, EAE 79 days after injection). Quantification of nestin-, OX42- and GFAP-immunostaining was performed in the ventral horn of the lumbar tract of the spinal cord. The quantitative results referring to the qualitative data described above are shown in Figure 3. With the exception of a small but significant microglial activation in adjuvant-injected animals, no differences were observed between uninjected and adjuvant-injected rats.

Motoneurone gene expression regulation

Large neurones in the ventral horn of the spinal cord express ChAT and CGRP mRNAs. Quantitative analysis of ChAT and CGRP mRNAs levels in single motoneurones in control animals and during EAE is shown in Figure 4. ChAT mRNA level declines in the acute stage of EAE and remains lower than in control animals in the remission phase. No differences between pathological and control animals were observed at the end of the experiment, which corresponds to a partial recovery from relapse. Conversely, CGRP mRNA level is higher in motoneurones in pathological animals in the acute phase of the disease. Finally, p75^{LNGFR}-IR, which is never observed in control animals, appears transiently in motoneurones of pathological animals 14 days after immunization (Figure 2**I–M**).

Discussion

In this study we showed that during the inflammatory-autoimmune disease EAE spinal motoneurones undergo phenotype changes involving ChAT, CGRP and p75 similar to those described following axonal lesion, which supports the view that long-lasting neurological disabilities are related to neurone alterations that follow demyelination. We also confirmed that a severe gliosis results from astrocyte hypertrophy and hyperplasy in EAE [1]. GFAP-IR cells surrounds the cell body and dendrites of spinal motoneurones during acute EAE, and we found that GFAP-immunostaining further increases after resolution of the acute phase.

While axonal damage has been indicated as one of the typical features of MS and EAE histopathology [3,15] ever since it was first described, the possibility of whole neurone damage being a possible substrate for both permanent motor disabilities and cognitive problems and degeneration has only emerged in recent years. Gene expression switching has been described in spinal motoneurones in response to axotomy and during regeneration [31,32]. Sciatic nerve axotomy produces a transient loss of ChAT mRNA, re-expression of p75^{LNGFR} [24] and increase in cellular content of CGRP and mRNA [33]. Demyelinating lesions located where motor roots emerge from the spinal cord cause axonal lesions in motor neurones [18]. We describe how a decrease in ChAT mRNA expression is linked to increased CGRP mRNA levels and the re-appearance of p75^{LNGFR}-IR in the acute stage of EAE. ChAT mRNA levels decrease concomitantly with dramatic microglial (OX42-IR) and astroglial activation, as described by nestin-IR. Nestin is recognized as an earlier marker for astrocytic activation than GFAP [34]. CGRP in motoneurone acts as cotransmitter for acetylcholine, enhancing its spontaneous release in skeletal muscle, but also has a perhaps prevalent trophic action [35]. The rise of CGRP-IR in deafferentiated motoneurones is generally attributed to increased synthesis, although accumulation because of the blocking of peripheral transport cannot be excluded [36,37]. The neurotrophin receptor p75^{LNGFR}, which binds NGF, brain-derived neurotrophic factor (BDNF), neurotrophin 3–4 (NT3–4) and tumour necrosis factor-α (TNF-α) [38], is expressed by developing motoneurones in the spinal cord, whereas in adult motoneurones it re-appears after lesions, including sciatic nerve

---

Figures 2. **A**, **B**: immunostaining for oligodendrocytes on the longitudinal section of the lumbar tract of the spinal cord in control (**A**) and EAE (**B**) animals, 79 days after injection; **C**, **D**: nestin-IR in longitudinal section of the lumbar tract of the spinal cord EAE animals 14 (**C**) and 21 (**D**) days after injection. **E**, **F**: GFAP-immunostating in the ventral horn of the spinal cord of control (**E**) and EAE (**F**) animals, 79 days after injection; **I–M**: p75^{LNGFR}-IR in spinal motoneurones of EAE animals 14 days after injection. **G**, **H**, **N**: nestin-IR elements in the spinal cord of EAE animals 14 days after injection. Bars: **A**, 250 μm; **E**, **I**, **G**: 50 μm.
EAE, experimental allergic encephalomyelitis; GFAP, glial fibrillary acid protein.
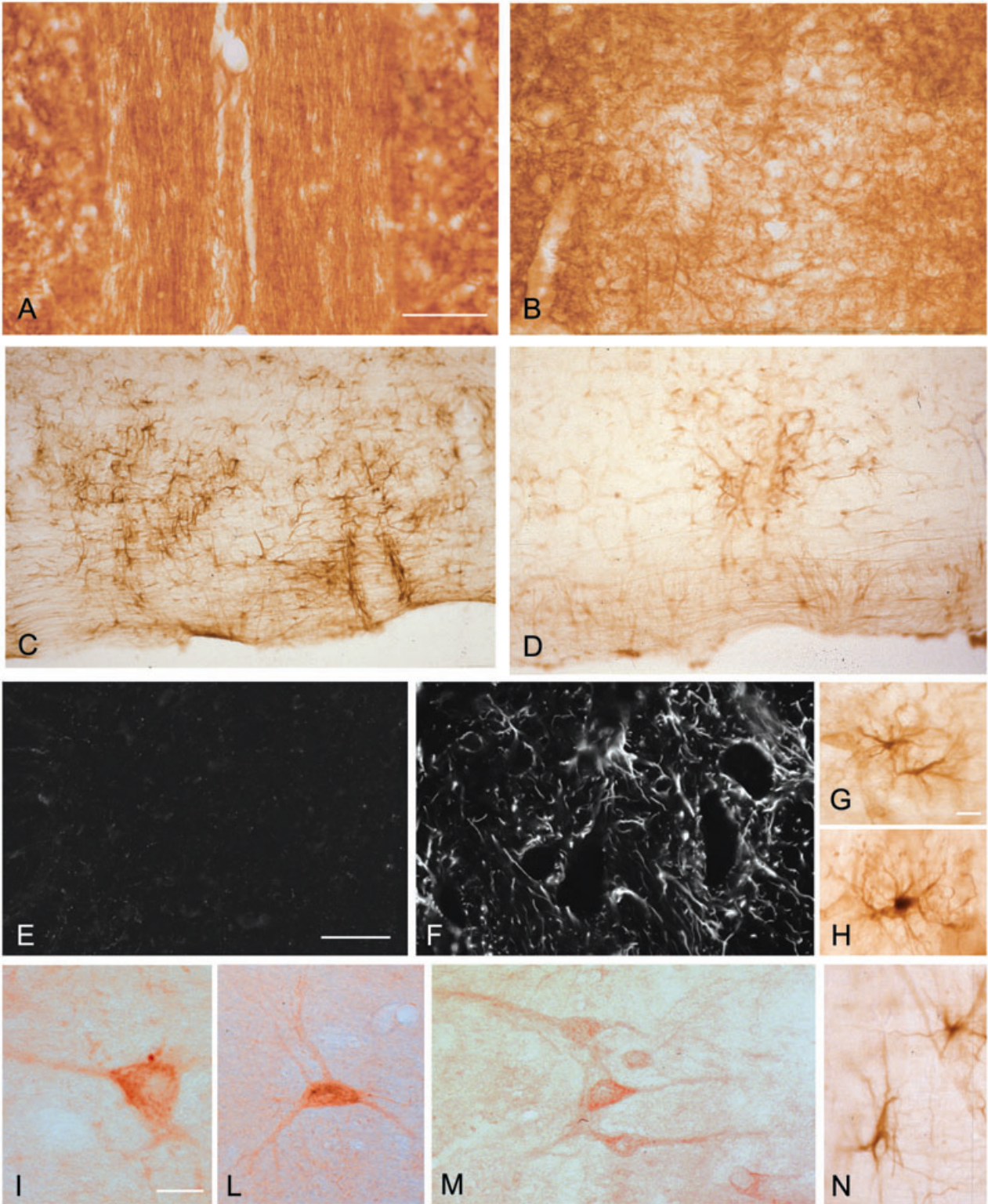
axotomy [39,40]. p75[LNGFR] has also been associated with cell death [41]. However, it is accepted that p75[LNGFR] upregulation possibly increases resistance to pathological motor neurone degeneration [42] and is present only in adult motor neurones that are allowed to regenerate [43].

Acute axonal damage is associated with an axonal conduction block, ion channel redistribution [20] and interruption of axoplasmic flow [44], including also trophic factors. We have already reported a dramatic drop in NGF content in the spinal cord during the acute phase of EAE and this defect could be involved in the clinical symptoms [30]. Indeed NGF administration attenuates neurological deficits in EAE marmosets [45,46], and ciliary neurotrophic factor (CNTF), which has been indicated as a major trophic factor for adult motoneurones, is a protective factor for severe neurological deficits in EAE [47]. Finally, a proper axonal function is required for successful remyelination in experimental pathologies [48]. Electrical activity in the axon is actually involved in regulating differentiation and the survival of oligodendrocyte precursors during development [49] and plays a key role in the induction of myelination [50].

Changes in neurochemical phenotype in spinal motoneurones could be related to the axonal damage at the point of emergence of the motor root in the extensive demyelinating regions present in the spinal cord during EAE, but also to other types of attack, for example, glutamate excitotoxicity, which is also related to permanent gliosis [51]. We found that immunostaining of an astrocyte marker protein such as GFAP clearly highlights the cell body and dendrites of motoneurones in layers 8 and 9 of the ventral horn of the spinal cord. Astrocytes in EAE animals actually have a decreased capacity to metabolize glutamate, as indicated by the severe decrease in the activity of specific enzymes [51]. Damage to dendrites and synapses occurs in motoneurones in inflamed spinal cord during EAE, as indicated by quantitative analysis of protein associated with these cell components [32]. Dendrite damage recovers significantly, although incompletely, during EAE remission [52], such as molecular indices of synaptic structures [53]. The temporal profile of alterations in dendrite and synapse damage in spinal cord correlates with the neurochemical changes we describe in the present study. In spite of the recovery, we cannot exclude that repeated inflammatory attacks or permanent gliosis may lead to permanent phenotype changes and even to motoneurone degeneration.
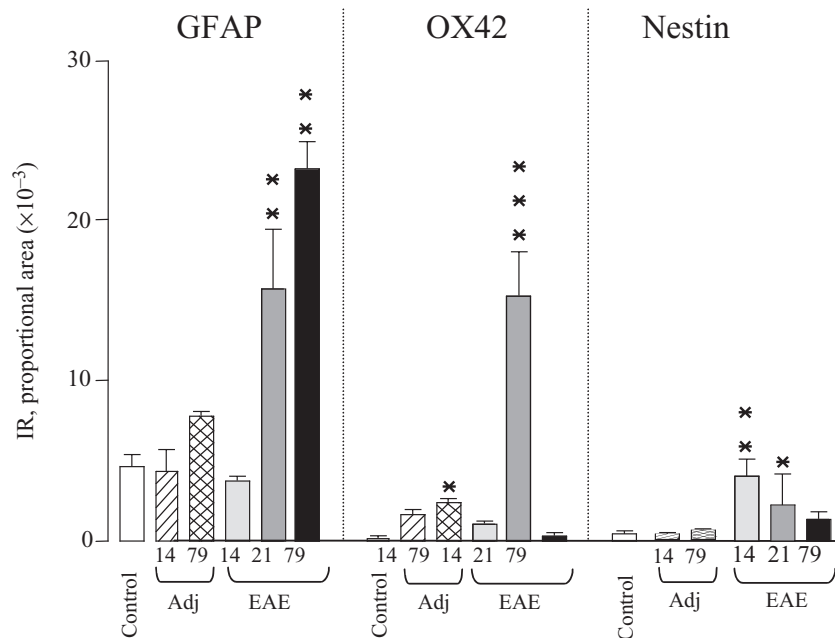
Figure 3. Quantitative evaluation of glial reaction in control and experimental animals at different times (14, 21 and 79 days) after immunization. GFAP, OX42 and nestin-IR were evaluated as an area covered by the immunoreactive signal in the area of the ventral horn of the spinal cord. Data area expressed as mean ± SEM. Statistical analysis: one-way ANOVA and Dunnett test, *$P < 0.05$, **$P < 0.01$, ***$P < 0.001$. Adj, adjuvant-injected; EAE, experimental allergic encephalomyelitis; GFAP, glial fibrillary acid protein.
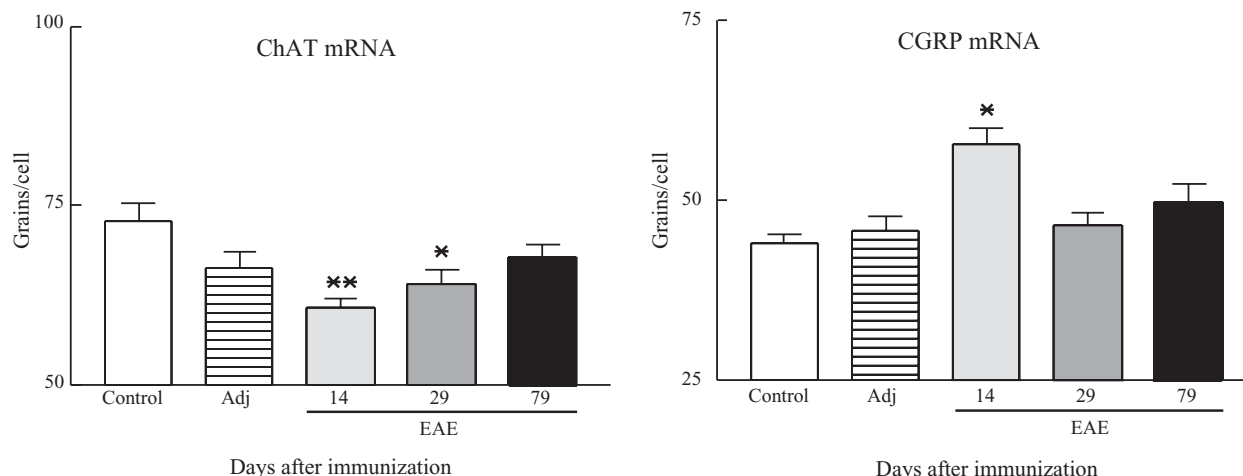
Figure 4. Quantitative analysis of ChAT and CGRP mRNA level in single cells in the ventral horn of the spinal cord at different times (14, 21 and 79 days) after immunization. Data area expressed as mean ± SEM. Statistical analysis: one-way ANOVA and Dunnett test, *$P < 0.05$, **$P < 0.01$.

Adj, adjuvant-injected; ChAT, choline acetyl-transferase; CGRP, calcitonin gene-related peptide.

Because of either axonal pathology resulting from demyelination and consequent neuronal stress, or a direct inflammatory attack on the cell body, modifications of the neurochemical phenotype in single spinal motoneurones observed in acute EAE indicate that severe motoneurone distress occurs in early phases of the disease. Our study was not designed to evaluate motoneurone cell number, so we cannot speculate as to whether recovery of normal neurochemical phenotype in single neurones means recovery in all neurones or only in surviving neurones. Recently, Smith *et al.* [54] described how motoneurones are subject to lymphocyte attack leading to a 30% reduction in neurone density in the ventral spinal cord in acute EAE. Neural cell loss has been indicated as one of the possible causes of brain and spinal cord atrophy in MS and EAE [55]. Apoptosis actually causes severe cell loss secondary to axonal damage in retinal ganglion cells during EAE [56] and it has been shown that cerebrospinal fluid from MS patients induces neuronal apoptosis *in vitro* [57]. Imaging studies have indicated that while normal brain atrophy is estimated at around 0.1–0.2% per year in normal subjects, it increases to approximately 1% in patients with progressive MS [58,59]. Brain and spinal cord atrophy is also a common feature in remittance-relapsing MS including also the spinal cord [60].

In conclusion, our data further suggest that distress, or lesion or degeneration of selective neural populations including cholinergic motoneurones in the spinal cord correlates with a temporal profile of neurological disability

of EAE and MS. Thus, not only axons, but also the whole neurone should be investigated in order to define a possible neuroprotective strategy to include in MS multitherapy [61].

Acknowledgements

References

1 Scolding NJ, Zajicek JP, Wood N, Compston DAS. The pathogenesis of demyelinating disease. *Prog Neurobiol* 1994; **43**: 143–73

2 Merrill JE, Scolding NJ. Mechanisms of damage to myelin and oligodendrocytes and their relevance to disease. *Neuropathol Appl Neurobiol* 1999; **25**: 435–58

3 Bitsch A, Schuchardt J, Bunkowski S, Kuhlmann T, Bruck W. Acute axonal injury in multiple sclerosis. Correlation with demyelination and inflammation. *Brain* 2000; **126**: 1174–83

4 Ferguson B, Matyszak MK, Esiri MM, Perry VH. Axonal damage in acute multiple sclerosis lesions. *Brain* 1997; **120**: 393–9

5 Ganter P, Prince C, Esiri MM. Spinal cord axonal loss in multiple sclerosis: a post-mortem study. *Neuropathol Appl Neurobiol* 1999; **25**: 459–67

6 Evangelou N, Konz D, Esiri MM, Smith S, Palace J, Matthews PM. Size-selective neuronal changes in the anterior

optic pathways suggest a differential susceptibility to injury in multiple sclerosis. *Brain* 2001; **124**: 1813–20

7　Bjartmar C, Yin X, Trapp BD. Axonal pathology in myelin disorders. *J Neurocytol* 1999; **28**: 383–95

8　Rieckmann P, Smith KJ. Multiple sclerosis: more than inflammation and demyelination. *Trends Neurosci* 2001; **24**: 435–7

9　Silber E, Sharief MK. Axonal degeneration in the pathogenesis of multiple sclerosis. *J Neurol Sci* 1999; **170**: 11–8

10　Arnold DL. Magnetic resonance spectroscopy: imaging axonal damage in MS. *J Neuroimmunol* 1999; **98**: 2–6

11　De Stefano N, Narayanan S, Matthews PM, Francis GS, Antel JP, Arnold DL. In vivo evidence for axonal dysfunction remote from focal cerebral demyelination of the type seen in multiple sclerosis. *Brain* 1999; **122**: 1933–9

12　De Stefano N, Narayanan S, Francis GS, Arnaoutelis R, Tartaglia MC, Antel JP, Matthews PM, Arnold DL. Evidence of axonal damage in the early stages of multiple sclerosis and its relevance to disability. *Arch Neurol* 2001; **58**: 65–70

13　De Stefano N, Narayanan S, Matthews PM, Mortilla M, Dotti MT, Federico A, Arnold DL. Proton MR spectroscopy to assess axonal damage in multiple sclerosis and other white matter disorders. *J Neurovirol* 2000; **2** (Suppl.): S121–9

14　Ciccarelli O, Werring DJ, Wheeler-Kingshott CA, Barker GJ, Parker GJ, Thompson AJ, Miller DH. Investigation of MS normal-appearing brain using diffusion tensor MRI with clinical correlations. *Neurology* 2001; **56**: 926–33

15　De Stefano N, Matthews PM, Fu L, Narayanan S, Stanley J, Francis GS, Antel JP, Arnold DL. Axonal damage correlates with disability in patients with relapsing-remitting multiple sclerosis. Results of a longitudinal magnetic resonance spectroscopy study. *Brain* 1998; **121**: 1469–77

16　Matthews PM, De Stefano N, Narayanan S, Francis GS, Wolinsky JS, Antel JP, Arnold DL. Putting magnetic resonance spectroscopy studies in context: axonal damage and disability in multiple sclerosis. *Semin Neurol* 1998; **18**: 327–36

17　Evangelou N, Konz D, Esiri MM, Smith S, Palace J, Matthews PM. Regional axonal loss in the corpus callosum correlates with cerebral white matter lesion volume and distribution in multiple sclerosis. *Brain* 2000; **123**: 1845–9

18　Kornek B, Storch MK, Bauer J, Djamshidian A, Weissert R, Wallstroem E, Stefferl A, Zimprich F, Olsson T, Linington C, Schmidbauer M, Lassmann H. Distribution of a calcium channel subunit in dystrophic axons in multiple sclerosis and experimental autoimmune encephalomyelitis. *Brain* 2001; **124**: 1114–24

19　Dandekar AA, Wu GF, Pewe L, Perlman S. Axonal damage is T cell mediated and occurs concomitantly with demyelination in mice infected with a neurotropic coronavirus. *J Virol* 2001; **75**: 6115–20

20　Kornek B, Storch MK, Weissert R, Wallstroem E, Stefferl A, Olsson T, Linington C, Schmidbauer M, Lassmann H. Multiple sclerosis and chronic autoimmune encephalomyelitis: a comparative quantitative study of axonal injury in active, inactive, and remyelinated lesions. *Am J Pathol* 2000; **157**: 267–76

21　Onuki M, Ayers MM, Bernard CC, Orian JM. Axonal degeneration is an early pathological feature in autoimmune-mediated demyelination in mice. *Microsc Res Tech* 2001; **52**: 731–9

22　Mancardi G, Hart B, Roccatagliata L, Brok H, Giunti D, Bontrop R, Massacesi L, Capello E, Uccelli A. Demyelination and axonal damage in a non-human primate model of multiple sclerosis. *J Neurol Sci* 2001; **184**: 41–9

23　Pouly S, Antel JP, Ladiwala U, Nalbantoglu J, Becher B. Mechanisms of tissue injury in multiple sclerosis: opportunities for neuroprotective therapy. *J Neural Transm* 2000; **58**: 193–203

24　Terenghi G. Peripheral nerve regeneration and neurotrophic factors. *J Anat* 1999; **194**: 1–14

25　Calza L, Giardino L, Giuliani A, Aloe L, Levi-Montalcini R. Nerve growth factor control of neuronal expression of angiogenetic and vasoactive factors. *Proc Natl Acad Sci USA* 2001; **98**: 4160–5

26　Giardino L, Giuliani A, Battaglia A, Carfagna N, Aloe L, Calzà L. Neuroprotection and aging of the cholinergic system: a role for the ergoline derivative nicergoline (Sermion). *Neuroscience* 2002; **109**: 487–97

27　Hickey W, Gonatas NK, Kimura H, Wilson DB. Identification and quantitation of T lymphocyte subsets found in the spinal cord of the Lewis rat during acute experimental allergic encephalomyelitis. *J Immunol* 1983; **131**: 2805–9

28　Pozza M, Bettelli C, Aloe L, Giardino L, Calza L. Further evidence for a role of nitric oxide in experimental allergic encephalomyelitis: aminoguanidine treatment modifies its clinical evolution. *Brain Res* 2000; **855**: 39–46

29　Dagerlind A, Friberg K, Bean AJ, Hokfelt T. Sensitive mRNA detection using unfixed tissue: combined radioactive and non-radioactive in situ hybridization histochemistry. *Histochemistry* 1992; **98**: 39–49

30　Calza L, Giardino L, Pozza M, Micera A, Aloe L. Timecourse changes of nerve growth factor, corticotropin-releasing hormone, and nitric oxide synthase isoforms and their possible role in the development of inflammatory response in experimental allergic encephalomyelitis. *Proc Natl Acad Sci USA* 1997; **94**: 3368–73

31　Wu W. Potential roles of gene expression change in adult rat spinal motoneurons following axonal injury: a comparison among c-jun, off-affinity nerve growth factor receptor (LNGFR), and nitric oxide synthase (NOS). *Exp Neurol* 1996; **141**: 190–200

32　Zhu B, Luo L, Moore GR, Paty DW, Cynader MS. Dendritic and synaptic pathology in experimental autoimmune encephalomyelitis. *Am J Pathol* 2003; **162**: 1639–50

33　Piehl F, Ji RR, Cullheim S, Hokfelt T, Lindholm D, Hughes RA. Fibroblast growth factors regulate calcitonin generelated peptide mRNA expression in rat motoneurons

after lesion and in culture. *Eur J Neurosci* 1995; **7**: 1739–50

34 Krum JM, Rosenstein JM. Transient coexpression of nestin, GFAP, and vascular endothelial growth factor in mature reactive astroglia following neural grafting or brain wounds. *Exp Neurol* 1999; **160**: 348–60

35 Arvidsson U, Piehl F, Johnson H, Ulfhake B, Cullheim S, Hokfelt T. The peptidergic motoneurone. *Neuroreport* 1993; **4**: 849–56

36 Arvidsson U, Johnson H, Piehl F, Cullheim S, Hokfelt T, Risling M, Terenius L, Ulfhake B. Peripheral nerve section induces increased levels of calcitonin gene-related peptide (CGRP)-like immunoreactivity in axotomized motoneurons. *Exp Brain Res* 1990; **79**: 212–6

37 Caldero J, Casanovas A, Sorribas A, Esquerda JE. Calcitonin gene-related peptide in rat spinal cord motoneurons: subcellular distribution and changes induced by axotomy. *Neuroscience* 1992; **48**: 449–61

38 Kaplan DR, Miller FD. Neurotrophin signal transduction in the nervous system. *Curr Opin Neurobiol* 2000; **10**: 381–91

39 Rende M, Hagg T, Manthorpe M, Varon S. Nerve growth factor receptor immunoreactivity in neurons of the normal adult rat spinal cord and its modulation after peripheral nerve lesions. *J Comp Neurol* 1992; **319**: 285–98

40 Rende M, Provenzano C, Tonali P. Modulation of low-affinity nerve growth factor receptor in injured adult rat spinal cord motoneurons. *J Comp Neurol* 1993; **338**: 560–74

41 Syroid DE, Maycox PJ, Soilu-Hanninen M, Petratos S, Bucci T, Burrola P, Murray S, Cheema S, Lee KF, Lemke G, Kilpatrick TJ. Induction of postnatal Schwann cell death by the low-affinity neurotrophin receptor in vitro and after axotomy. *J Neurosci* 2000; **20**: 5741–7

42 Seeburger JL, Springer JE. Experimental rationale for the therapeutic use of neurotrophins in amyotrophic lateral sclerosis. *Exp Neurol* 1993; **124**: 64–72

43 Bussmann KA, Sofroniew MV. Re-expression of p75NTR by adult motor neurons after axotomy is triggered by retrograde transport of a positive signal from axons regrowing through damaged or denervated peripheral nerve tissue. *Neuroscience* 1999; **91**: 273–81

44 Povlishock JT. Traumatically induced axonal injury: pathogenesis and pathological implications. *Brain Pathol* 1992; **2**: 1–12

45 Ransohoff RM, Trebst C. Surprising pleiotropy of nerve growth factor in the treatment of experimental autoimmune encephalomyelitis. *J Exp Med* 2000; **191**: 1625–30

46 Villoslada P, Hauser SL, Bartke I, Unger J, Heald N, Rosenberg D, Cheung SW, Mobley WC, Fisher S, Genain CP. Human nerve growth factor protects common marmosets against autoimmune encephalomyelitis by switching the balance of T helper cell type 1 and 2 cytokines within the central nervous system. *J Exp Med* 2000; **191**: 1799–806

47 Linker RA, Maurer M, Gaupp S, Martini R, Holtmann B, Giess R, Rieckmann P, Lassmann H, Toyka KV, Sendtner M, Gold R. CNTF is a major protective factor in demyelinating CNS disease: a neurotrophic cytokine as modulator in neuroinflammation. *Nat Med* 2002; **8**: 620–4

48 Levine JM, Reynolds R, Fawcett JW. The oligodendrocyte precursor cell in health and disease. *Trends Neurosci* 2001; **24**: 39–47

49 Barres BA, Raff MC. Control of oligodendrocyte number in the developing rat optic nerve. *Neuron* 1994; **12**: 935–42

50 Demerens C, Stankoff B, Logak M, Anglade P, Allinquant B, Couraud F, Zalc B, Lubetzki C. Induction of myelination in the central nervous system by electrical activity. *Proc Natl Acad Sci USA* 1996; **93**: 9887–92

51 Hardin-Pouzet H, Krakowski M, Bourbonniere L, Didier-Bazes M, Tran E, Owens T. Glutamate metabolism is down-regulated in astrocytes during experimental allergic encephalomyelitis. *Glia* 1997; **20**: 79–85

52 Hammarberg H, Lidman O, Lundberg C, Eltayeb SY, Gielen AW, Muhallab S, Svenningsson A, Linda H, van der Meide PH, Cullheim S, Olsson T, Piehl F. Neuroprotection by encephalomyelitis. Rescue of mechanically injured neurons and neurotrophin production by CNS-infiltrating T and natural killer cells. *J Neuroscience* 2000; **20**: 5283–91

53 Sandyk R. Serotonergic neuronal sprouting as a potential mechanism of recovery in multiple sclerosis. *Int J Neurosci* 1999; **97**: 131–8

54 Smith T, Groom A, Zhu B, Turski L. Autoimmune encephalomyelitis ameliorated by AMPA antagonists. *Nature Med* 2000; **6**: 62–6

55 Peterson JW, Bo L, Mork S, Chang A, Trapp BD. Transected neuritis, apoptotic neurons, and reduced inflammation in cortical multiple sclerosis lesions. *Ann Neurol* 2001; **50**: 389–400

56 Meyer R, Weissert R, Diem R, Storch MK, de Graaf KL, Kramer B, Bahr M. Acute neuronal apoptosis in a rat model of multiple sclerosis. *J Neurosci* 2001; **21**: 6214–20

57 Cid C, Alcazar A, Regidor I, Masjuaan J, Salinas M, Alvarez-Cermeno JC. Neuronal apoptosis induced by cerebrospinal fluid from multiple sclerosis patients correlates with hypointense lesions on T1 magnetic resonance imaging. *J Neurol Sci* 2002; **193**: 103–9

58 Bjartmar C, Trapp BD. Axonal and neuronal degeneration in multiple sclerosis: mechanisms and functional consequences. *Curr Opin Neurol* 2001; **14**: 271–8

59 Chard DT, Griffin CM, Parker GJ, Kapoor R, Thompson AJ, Miller DH. Brain atrophy in clinically early relapsing-remitting multiple sclerosis. *Brain* 2002; **125**: 327–37

60 Simon JH. Brain and spinal cord atrophy in multiple sclerosis: role as a surrogate measure of disease progression. *CNS Drugs* 2001; **15**: 427–36

61 Steinman L. Multiple approaches to multiple sclerosis. *Nat Med* 2000; **6**: 15–6